Applied Problems of Nonlinear Oscillation and Wave Theory

Izvestiya Vysshikh Uchebnykh Zavedeniy. Applied Nonlinear Dynamics. 2023;31(5)

Article DOI: 10.18500/0869-6632-003059

Mathematical model of the photoplethysmogram for testing methods of biological signals analysis

A. M. Vakhlaeva✉, *Yu. M. Ishbulatov, A. S. Karavaev, V. I. Ponomarenko, M. D. Prokhorov*

Saratov Branch of Kotelnikov Institute of Radioengineering and Electronics of the RAS, Russia
E-mail: ✉vakhlaeva.anna@gmail.com, ishbulatov95@mail.ru, karavaevas@gmail.com, ponomarenkovi@gmail.com, mdprokhorov@yandex.ru

Received 15.05.2023, accepted 22.06.2023, available online 19.09.2023, published 29.09.2023

Abstract. The *purpose* of this study was to develop a mathematical model of the photoplethysmogram, which can be used to test methods that introduce the instantaneous phases of the modulating signals. The model must reproduce statistical and spectral characteristics of the real photoplethysmogram, and explicitly incorporate the instantaneous phases of the modulating signals, so they can be used as a reference during testing. *Methods.* Anacrotic and catacrotic phases of the photoplethysmogram pulse wave were modeled as a sum of two density distributions for the skew normal distribution. The modulating signals were introduced as harmonic functions taken from the experimental instantaneous phases of the VLF (0.015...0.04 Hz), LF (0.04...0.15 Hz) and HF (0.15...0.4 Hz) oscillations in the real photoplethysmogram. The spectral power in the VLF, LF, and HF frequency ranges was calculated to compare the model and experimental data. *Results.* The model qualitatively reproduces the shape of the experimental photoplethysmogram pulse wave and shows less than 1% error when simulating the spectral properties of the signal. *Conclusion.* The proposed mathematical model can be used to test the methods for introduction of the instantaneous phases of the modulating signals in photoplethysmogram time-series.

Keywords: mathematical modeling, photoplethysmogram, phase analysis, spectral analysis, synchronization, directional coupling.

Acknowledgements. The work was carried out within the framework of the state task of the Saratov Branch of the Institute of Radioengineering and Electronics of Russian Academy of Sciences.

For citation: Vakhlaeva AM, Ishbulatov YuM, Karavaev AS, Ponomarenko VI, Prokhorov MD. Mathematical model of the photoplethysmogram for testing methods of biological signals analysis. Izvestiya VUZ. Applied Nonlinear Dynamics. 2023;31(5):586–596. DOI: 10.18500/0869-6632-003059

Introduction

The approach to the study of the cardiovascular system, based on the application of methods of radiophysics and nonlinear dynamics, proved to be extremely fruitful and allowed us to obtain a number of fundamental and applied results. Complexity measures [1], spectral characteristics [2], as well as quantitative characteristics of directional coupling [3] and synchronization [4], applied to the analysis of the cardiovascular system signals, are used to diagnose and control therapy of socially significant diseases, including hypertension [2] and diabetes [5]. These approaches are also used to diagnose stress [6, 7], solving problems of sports medicine [8] and fundamental study of the dynamics of interaction of various elements of the cardiovascular system during active experiments [9], various stages of sleep [10], etc.

When studying the cardiovascular system signals, many authors consider the system of autonomous regulation of blood circulation in the form of an ensemble of interacting self-oscillating systems with a delay in feedback loops. Registration of photoplethysmograms (PPG) is a non-invasive and affordable way to assess the self-oscillatory dynamics of the contours of autonomous regulation, including sympathetic and parasympathetic regulation of vascular tone and sympathetic regulation of heart rhythm [11]. The wide availability of wearable commercial PPG recorders further spurs interest in the study of this signal [12]. However, the analysis of PPG, as well as the analysis of any signals of biological origin, is complicated by their unsteadiness, broadband spectral composition and the presence of color noise. The listed factors acutely pose the problem of testing and parametrization of methods of phase introduction, detection of phase synchronization, diagnostics of directional connections, etc., etc. Analysis of exclusively experimental data cannot provide unambiguous solutions to the listed problems. For experimental data, the correct result is not known, for example, the true shape of the time series of the instantaneous phase or the values of the coupling coefficients are not known. It makes it impossible to quantify the accuracy of estimations obtained using the given set of parameters.

A typical solution to these difficulties is to test the methods on the mathematical models, which have a rich history of development. There are classical reference systems, as well as low-dimensional models of low-frequency rhythms of PPG in the form of first-order differential equations with a delay in feedback loops [13], which are certainly necessary at the initial stages of testing, but do not simulate the complex broadband spectral composition of real data. There are models reproducing the shape of oscillations in biological signals [14, 15], such models are adapted to the data of specific patients. From the first principles, multicomponent models [16] are proposed, reproducing the structure and complex dynamics of the the cardiovascular system and synthesizing signals that qualitatively correspond to real signals in terms of spectral and statistical characteristics. However, we have not found models in which the instantaneous phases of the signals of the modulation of the PPG signal and the frequency modulation of the main heart rhythm would be set explicitly and could be directly extracted from the mathematical model. Thus, the listed models cannot provide the reference time series of the instantaneous phase difference required during testing and comparison of various methods of phase introduction. Therefore, the purpose of this work was to develop a simulation mathematical model of the PPG signal, in which the instantaneous phases of the modulation signals are present explicitly. In addition, a necessary condition was to achieve a quantitative correspondence of the spectral and phase characteristics of the model and real signals, as well as the the correspondence between the shapes of the model and experimental time series.

1. Mathematical model

The developed mathematical model is based on the approaches proposed in [14] and [15]. The main heart rate was set by the time of one pass of the mapping point along the limit cycle, to which the phase trajectory of the next dynamic system converged:

$$\begin{cases} \dot{x}\ (t) = \alpha x(t) - \omega(t) y(t), \\ \dot{y}\ (t) = \alpha y(t) + \omega(t) x(t), \end{cases} \tag{1}$$

where

$$\omega\ (t) = 2\pi\ / \Big(w_0 + \sum_{i=\mathrm{VLF,LF,HF}} k_i^{\mathrm{HRV}} \cos\left(\varphi_i^{\mathrm{HRV}}(t)\right) \Big). \tag{2}$$

In the formula (1) $\alpha = 1 - \sqrt{x^2(t) + y^2(t)}$, in the formula (2) $\varphi_i^{\mathrm{HRV}}(t)$ are instantaneous phases of Heart Rate Variability (HRV) registered in the field experiment in VLF (0.015...0.04 Hz), LF (0.04...0.15 Hz) and HF (0.15...0.4 Hz) frequency ranges, ω_0 is the natural frequency of the main heart rate, k_i^{HRV} are dimensionless coefficients that determine the depth of frequency modulation in the VLF, LF and HF bands. The equations (1) and (2) were solved by the 4th-order Runge-Kutta method with an integration step of 0.004. The shape of the pulse wave of the PPG within a separate cardiocycle was described by the expression:

$$\mathrm{PPG}(t) = \sum_{i=\mathrm{VLF,LF,HF}} k_i^{\mathrm{PPG}} \cos\left(\varphi_i^{\mathrm{PPG}}(t)\right) + 2 \sum_{i=\mathrm{An,Cat}} a_i \gamma_i(t) \Gamma_i(t), \tag{3}$$

where $\varphi_i^{\mathrm{PPG}}(t)$ are instantaneous oscillation phases of experimental PPG in VLF (0.015...0.04 Hz), LF (0.04...0.15 Hz) and HF (0.15...0.4 Hz) frequency ranges. k_i^{PPG} are dimensionless coefficients determining the modulation depth in the VLF, LF and HF bands. The expression under the last sign of the sum is a function that conveys the shape of the density of an asymmetric normal distribution. The sum of two such expressions qualitatively corresponds to the typical type of pulse wave of the PPG, which is the sum of anacrotic and catacrotic phases. The subscripts An and Cat denote parameters and expressions related, respectively, to the anacrotic and catacrotic phases of the PPG. The parameters a_i, where $i = \mathrm{An, Cat}$, determine the height of the anacrotic and catacrotic phases of the PPG. The notation $\gamma_i(t)$ and $\Gamma_i(t)$, where $i = \mathrm{An, Cat}$, corresponded to the expressions (4) и (5):

$$\gamma_i(t) = \frac{1}{b_i\sqrt{2\pi}} e^{\left(s_i \left(\frac{T_n(t) - T_i}{b_i}\right)^2\right)}, \tag{4}$$

$$\Gamma_i(t) = \int \gamma_i(t), \tag{5}$$

in which s_i, b_i, T_i, where $i = \mathrm{An, Cat}$ are parameters, respectively, of the asymmetry, width and position of the anacrotic $i = \mathrm{An}$ and catacrotic $i = \mathrm{Cat}$ of the PPG phases, $T_n(t)$ is a function that depends non-linearly on the time elapsed since the beginning of the cardiocycle, $T(t)$. The time $T(t)$ was given by a trivial model of accumulation and reset $\dot{T}(t) = 1$, where $T(t)$ was reduced to 0, when the instantaneous phase of the main heart rate $\varphi(t)$ reached 1, this instantaneous phase was introduced as $\varphi(t) = \mathrm{arctg}\left(y(t)/x(t)\right)$. The first 0.5 s from the beginning of the cardiocycle, which accommodate anacrotic and catacrotic phases, $T_n(t) = T(t)$. After 0.5 s, the function $T_n(t)$, in general, increased linearly faster or slower than $T(t)$, according to the equation (6), and reached 1 by the end of the cardiocycle.

$$\dot{T}_n(t) = \frac{0.5}{T_c - 0.5}, \tag{6}$$

where T_c is the duration of the current cardiocycle. The equation (6) ensured that the function reached $T_n(t)$ units for the remainder of the cardiocycle. The final stage was smoothing the dependence of $T_n(t)$ with a moving average filter with a window width of 31 discrete time counts. Introduction of the function $T_n(t)$ due to the need to achieve two goals: the first is the need to maintain the constancy of the time interval between the beginning of the cardiocycle and the peak of the anacrotic phase; the second is the elongation of the pulse wave in the case of long cardiocycles and its narrowing in the case of short cycles. If we rewrite the equation (4) using directly the phase $\varphi(t)$, then the pulse wave will lengthen and shorten depending on the duration of the cardiocycle, but at the same time the time interval between the beginning of the cycle and anacrotic rise will also change. This would lead to significant errors in the estimation of heart rate variability as a sequence of time intervals between anacrotic rises of pulse waves of PPG, which contradicts experimental observations, at least for patients without pronounced pathologies [17]. If we rewrite the expression (4) using $T(t)$ instead of $T_n(t)$, the pulse wave duration will remain constant and will cease to correspond to the duration of the cardiac cycle.

When generating the model implementations presented in the section «Results», instantaneous phases of VLF, LF and HF oscillations were used from two-hour recordings of RR intervals (sequences of time intervals between ECG R-waves) and signals of blood filling of the finger vessels of five healthy subjects aged 19 to 21 years. The signals were registered by an infrared optical sensor with active illumination in reflected light (PPG). The fluctuations of the VLF, LF and HF ranges were extracted from the PPG signals using rectangular bandpass filters with passbands, respectively, 0.015...0.04 Hz, 0.04...0.15 Hz and 0.15...0.4 Hz. The extraction of VLF, LF and HF band oscillations from the RR interval signals was performed in a similar way, but before filtering, the signal was interpolated with cubic β splines and re-sampled with a sampling frequency of 250 Hz. The instantaneous phases were then introduced using the Hilbert transform.

The parameters of the mathematical model that determine the shape of the PPG signal oscillations within a separate cardiocycle were selected in such a way as to achieve a qualitative correspondence to the typical form of experimental signals of healthy volunteers. The parameters k_i^{HRV}, where $i =$ VLF, LF and HF, were selected separately for each time implementation of the mathematical model generated using the instantaneous phases VLF, LF and HF fluctuations of RR intervals and PPG of a particular healthy volunteer. The parameters were selected using an iterative procedure that provided a quantitative correspondence (with an error of less than 1%) between the spectral power density in the VLF, LF and HF ranges of the experimental signal of the RR intervals and the sequence of time intervals between anacrotic rises of the model PPG.

The parameters k_i^{PPG}, where $i =$ VLF, LF and HF, were selected using a similar iterative procedure, which provided a quantitative correspondence (with an error of less than 1%) between the relative indices VLF_n, LF_n and HF_n, estimated for model and experimental PPG signals. The indices VLF_n, LF_n and HF_n were calculated as the spectral power density in the VLF, LF and HF ranges, respectively, normalized for power in the range [$\omega_0-0.1$ Hz, $\omega_0 + 0.1$ Hz], where ω_0 is average frequency heart rate, detected to the maximum in the power spectrum of the experimental PPG signal. This value ω_0 was also used in the system of equations (1). The model parameters are listed in the Table. Parameter values k_i^{HRV} and k_i^{PPG}, which brought the models in line with the data of specific

Table. Parameters of the mathematical model

Parameter	Meaning
a_{An}	60
a_{Cat}	10
T_{An}	0.06
T_{Cat}	0.35
b_{An}	0.22
b_{Cat}	0.15
S_{An}	10
S_{Cat}	5
ω_0	1.180 ± 0.188
$k_{\mathrm{VLF}}^{\mathrm{HRV}}$	3.954 ± 1.879
$k_{\mathrm{LF}}^{\mathrm{HRV}}$	4.499 ± 2.652
$k_{\mathrm{HF}}^{\mathrm{HRV}}$	1.250 ± 0.509
$k_{\mathrm{VLF}}^{\mathrm{PPG}}$	0.041 ± 0.014
$k_{\mathrm{LF}}^{\mathrm{PPG}}$	0.024 ± 0.003
$k_{\mathrm{HF}}^{\mathrm{PPG}}$	0.040 ± 0.012

patients and were unique for each implementation of the model, are presented as an average value plus/minus the standard deviation.

Experimental data were recorded by a standard certified EEG-21/26 polyregister "Encephalan-131-03" (LLC "Medikom-MTD", Taganrog). The bandwidth was 0.015...100 Hz at a sampling rate of 250 Hz and a resolution of — 14 bits. The ECG signal was recorded in the I standard Eithoven lead (differential signal from the wrists of two hands), the PPG signal was recorded from the distal phalanx of the ring finger of the right hand. The data were recorded in a lying position, in a calm environment, at a constant comfortable temperature.

2. Results

In Fig. 1 presents time series, power spectra and instantaneous phases of the modulation signal of the mean value of the PPG for a specific time implementation of the proposed mathematical model and a specific volunteer whose data were used in generating the depicted model signals.

From Fig. 1, *a* it can be seen that the shape of the model pulse wave qualitatively corresponds to experimental data, the model also conveys the presence of pronounced low-frequency trends. Fig. 1, *b*, *c* demonstrate a good quantitative correspondence between the power spectra of the model and experimental PPG signals. The mathematical model reproduces the spectral power density in the VLF, LF and HF frequency ranges with an error of less than 1%.

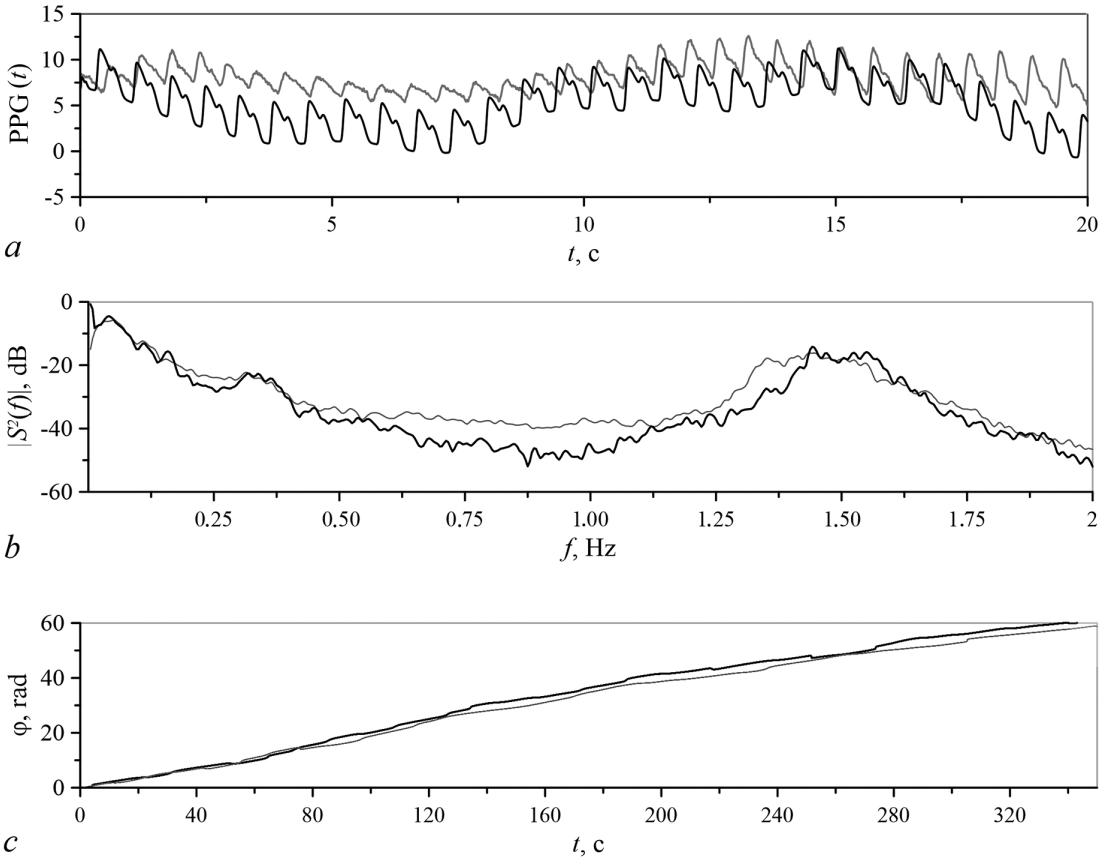

Fig 1. Time series (*a*), power spectra (*b*), and instantaneous phases (*c*) of the LF-oscillations (0.04...0.15 Hz) in the experimental (gray) and model (black) PPG signals

The model reproduces a characteristic peak in the center of the LF range at a frequency of about 0.1 Hz, associated with modulation of arterial vascular tone from the sympathetic link of the autonomous circulatory regulation system; peak in the HF range at a frequency of about 0.3 Hz, associated with the activity of the parasympathetic link of the regulation system and respiration; peak corresponding to the main heart rhythm. The model conveys the broadband nature of the real spectrum, as well as the presence of a $1/f$ pedestal associated with noise of central origin [18]. In Fig. 1, *c* the instantaneous phases of LF oscillations of the mean value of the PPG signal are presented. The gray solid line corresponds to the time realization of the variable $\varphi_{\mathrm{LF}}^{\mathrm{PPG}}(t)$ from the equation (3) and, thus, is equivalent to the true modulation signal in this frequency range. The black line corresponds to the empirical evaluation of this modulation signal based on the time implementation of the PPG model. The LF-band oscillations were isolated from the PPG signal using a rectangular bandpass filter with a bandwidth of 0.04...0.15 Hz, the oscillation phases were introduced in a classical way based on the Hilbert transform. From Fig. 1, *c* it can be seen that the average rate of rise of the instantaneous phase $\varphi_{\mathrm{LF}}^{\mathrm{PPG}}(t)$ and its estimates coincide, but the waveforms themselves differ, which can lead to errors in estimating the strength of directional bonds and synchronization diagnostics. The proposed mathematical model makes it possible to isolate and quantify the role of potential sources of errors, the presence of which is obvious from Fig. 1, *c*.

Fig. 2 illustrates the case of disabling the frequency modulation of the main heart rhythm. The graphs compare the averaged spectra of model PPG signals. The spectrum depicted in gray was obtained for models whose parameters were selected according to the procedure described in the previous section. The spectrum represented in black was obtained for models with the same parameters, except for the parameters k_i^{HRV}, which were reduced to zero. From Fig. 2 it can be seen that the peaks corresponding to the main heart rate of individual subjects have become narrower. There is also a slight decrease in the average power density in the VLF, LF and HF frequency ranges, which indicates the leakage of the heart rate frequency modulation signal into the low-frequency range of the PPG signal and allows us to expect that broadband heart rate modulation introduces errors when introducing instantaneous phases. The study of the implementations of the model with the frequency modulation of the heart rate disabled will allow us to estimate the errors in the introduction of phases due to errors in the parameterization of methods and the broadband nature of the modulation signal of the mean value of the PPG.

In Fig. 3 shows a case with disabled modulation of the PPG signal ($k_i^{\mathrm{PPG}} = 0$). It can be seen from the spectrum that spectral components remain in the VLF, LF and HF frequency ranges due to the presence of modulation of the main heart rhythm. The analysis

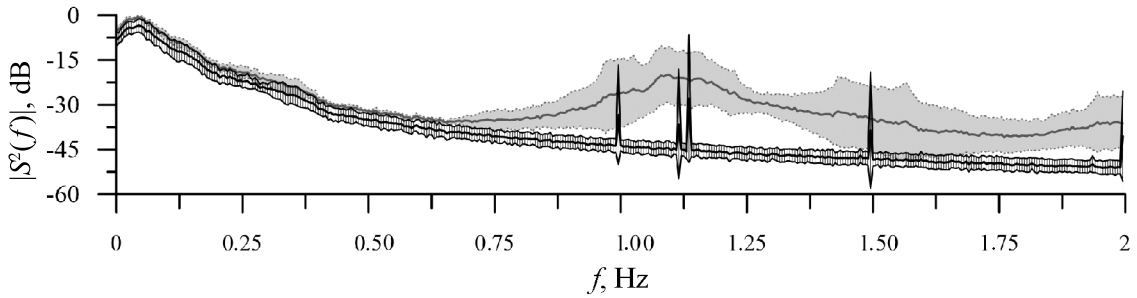

Fig 2. The gray line and its surrounding gray area correspond to the mean value and standard deviation of the model PPG power spectra, with parameters of the model set to simulate healthy individuals. The black plot with vertical black lines corresponds to the mean value and standard deviation of the model PPG power spectra, without the heart rate modulation

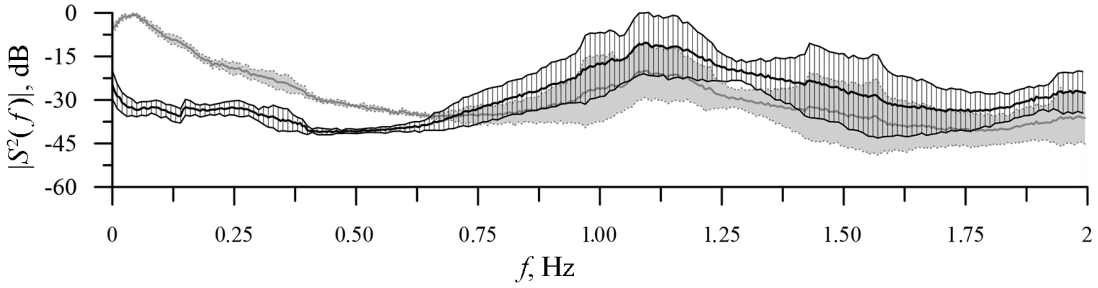

Fig 3. The gray line and its surrounding gray area correspond to the mean value and standard deviation of the model PPG power spectra, with parameters of the model set to simulate healthy individuals. The black plot with vertical black lines correspond to the mean value and standard deviation of the model PPG power spectra, without the modulation in the PPG signal

of the implementation of these mathematical models allows us to quantitatively investigate the effect of broadband heart rate modulation on the accuracy of the introduction of instantaneous phases of low-frequency oscillations of the PPG. This makes it possible to determine the limits of the applicability of the analysis methods and facilitates the interpretation of the results.

Conclusion

The paper presents a simulation mathematical model of the PPG signal, which provides a good quantitative correspondence to time series, instantaneous phases and power spectra of real PPG signals. The model has the functionality of adding frequency modulation of the main heart rate and the average value of the PPG in the form of oscillations with frequencies within the VLF, LF and HF ranges. The modulating signals are generated as a harmonic functions of the instantaneous phases of the VLF, LF and HF oscillations. Thus, the instantaneous phases of the modulation signals are present in the model explicitly, which makes it possible to use their time series as benchmarks for testing and comparing the accuracy of various methods of introducing instantaneous phases over time series. When generating a model using instantaneous phases of VLF, LF and HF oscillations extracted from the PPG and RR-intervals time series of the specific volunteer, the model can be personalized for that particular volunteer. In that case, the model provides quantitative correspondence to the real signal, with power in the VLF, LF, and HF ranges of model PPG and RR-intervals signals deviating from the experimental data by less than 1%.

References

1. Gorshkov O, Ombao H. Multi-chaotic analysis of inter-beat (R-R) intervals in cardiac signals for discrimination between normal and pathological classes. Entropy (Basel). 2021; 23(1):112. DOI: 10.3390/e23010112.
2. Fagard RH, Stolarz K, Kuznetsova T, Seidlerova J, Tikhonoff V, Grodzicki T, Nikitin Y, Filipovsky J, Peleska J, Casiglia E, Thijs L, Staessen JA, Kawecka-Jaszcz K. Sympathetic activity, assessed by power spectral analysis of heart rate variability, in white-coat, masked and sustained hypertension versus true normotension. J. Hypertens. 2007;25(11):2280–2285. DOI: 10.1097/HJH.0b013e3282efc1fe.
3. Borovkova EI, Prokhorov MD, Kiselev AR, Hramkov AN, Mironov SA, Agaltsov MV, Ponomarenko VI, Karavaev AS, Drapkina OM, Penzel T. Directional couplings between the respiration and parasympathetic control of the heart rate during sleep and wakefulness in healthy subjects at different ages. Front. Netw. Physiol. 2022;2:942700. DOI: 10.3389/fnetp.2022.942700.

4. Ponomarenko VI, Prokhorov MD, Karavaev AS, Kiselev AR, Gridnev VI, Bezruchko BP. Synchronization of low-frequency oscillations in the cardiovascular system: Application to medical diagnostics and treatment. The European Physical Journal Special Topics. 2013;222(10):2687–2696. DOI: 10.1140/epjst/e2013-02048-1.
5. Lefrandt JD, Smit AJ, Zeebregts CJ, Gans ROB, Hoogenberg KH. Autonomic dysfunction in diabetes: a consequence of cardiovascular damage. Current Diabetes Reviews. 2010;6(6): 348–358. DOI: 10.2174/157339910793499128.
6. Dimitriev DA, Saperova EV, Dimitriev AD. State anxiety and nonlinear dynamics of heart rate variability in students. PLoS ONE. 2016;11(1):e0146131. DOI: 10.1371/journal.pone.0146131.
7. Deka B, Deka D. Nonlinear analysis of heart rate variability signals in meditative state: a review and perspective. BioMedical Engineering OnLine. 2023;22(1):35. DOI: 10.1186/s12938-023-01100-3.
8. de Abreu RM, Porta A, Rehder-Santos P, Cairo B, Sakaguchi CA, da Silva CD, Signini ÉF, Milan-Mattos JC, Catai AM. Cardiorespiratory coupling strength in athletes and non-athletes. Respiratory Physiology & Neurobiology. 2022;305:103943. DOI: 10.1016/j.resp.2022.103943.
9. Delliaux S, Ichinose M, Watanabe K, Fujii N, Nishiyasu T. Muscle metaboreflex activation during hypercapnia modifies nonlinear heart rhythm dynamics, increasing the complexity of the sinus node autonomic regulation in humans. Pflügers Archiv - European Journal of Physiology. 2023;475(4):527–539. DOI: 10.1007/s00424-022-02780-x.
10. Karavaev AS, Skazkina VV, Borovkova EI, Prokhorov MD, Hramkov AN, Ponomarenko VI, Runnova AE, Gridnev VI, Kiselev AR, Kuznetsov NV, Chechurin LS, Penzel T. Synchronization of the processes of autonomic control of blood circulation in humans is different in the awake state and in sleep stages. Front. Neurosci. 2022;15:791510. DOI: 10.3389/fnins.2021.791510.
11. Goldstein DS, Bentho O, Park MY, Sharabi Y. Low-frequency power of heart rate variability is not a measure of cardiac sympathetic tone but may be a measure of modulation of cardiac autonomic outflows by baroreflexes. Exp. Physiol. 2011;96(12):1255–1261. DOI: 10.1113/expphysiol.2010.056259.
12. Natarajan A, Pantelopoulos A, Emir-Farinas H, Natarajan P. Heart rate variability with photoplethysmography in 8 million individuals: a cross-sectional study. The Lancet Digital Health. 2020;2(12):E650–E657. DOI: 10.1016/S2589-7500(20)30246-6.
13. Ringwood JV, Malpas SC. Slow oscillations in blood pressure via a nonlinear feedback model. American Journal of Physiology-Regulatory, Integrative and Comparative Physiology. 2001;280(4):R1105–R1115. DOI: 10.1152/ajpregu.2001.280.4.R1105.
14. Tang Q, Chen Z, Ward R, Elgendi M. Synthetic photoplethysmogram generation using two Gaussian functions. Sci. Rep. 2020;10(1):13883. DOI: 10.1038/s41598-020-69076-x.
15. McSharry PE, Clifford GD, Tarassenko L, Smith LA. A dynamical model for generating synthetic electrocardiogram signals. IEEE Transactions on Biomedical Engineering. 2003; 50(3):289–294. DOI: 10.1109/TBME.2003.808805.
16. Cheng L, Khoo MCK. Modeling the autonomic and metabolic effects of obstructive sleep apnea: a simulation study. Front. Physiol. 2012;2:111. DOI: 10.3389/fphys.2011.00111.
17. Mejía-Mejía E, May JM, Torres R, Kyriacou PA. Pulse rate variability in cardiovascular health: a review on its applications and relationship with heart rate variability. Physiol. Meas. 2020;41(7):07TR01. DOI: 10.1088/1361-6579/ab998c.
18. Kotani K, Struzik ZR, Takamasu K, Stanley HE, Yamamoto Y. Model for complex heart rate dynamics in health and diseases. Phys. Rev. E. 2005;72(4):041904. DOI: 10.1103/PhysRevE.72.041904.